Research Article Vol. 6, No. 3 / March 2019 / Optica 257

Optimal simultaneous measurements of incompatible observables of a single photon

Adetunmise C. Dada,[1,*] Will McCutcheon,[1] Erika Andersson,[2] Jonathan Crickmore,[2] Ittoop Puthoor,[2] Brian D. Gerardot,[2] Alex McMillan,[1] John Rarity,[1] and Ruth Oulton[1]

[1]Centre for Quantum Photonics, H. H. Wills Physics Laboratory and Department of Electrical and Electronic Engineering, University of Bristol, Bristol, BS8 1TL, UK
[2]Institute for Photonics and Quantum Sciences, SUPA, Heriot-Watt University, Edinburgh EH14 4AS, UK
*Corresponding author: tunmisedada@gmail.com

Received 20 August 2018; revised 2 December 2018; accepted 29 January 2019 (Doc. ID 340178); published 27 February 2019

The ultimate limits of measurement precision are dictated by the laws of quantum mechanics. One of the most fascinating results is that joint or simultaneous measurements of noncommuting quantum observables are possible at the cost of increased *unsharpness* or measurement uncertainty. Many different criteria exist for determining what an "optimal" joint measurement is, with corresponding different trade-off relations for the measurements. It is generally a nontrivial task to devise or implement a strategy that minimizes the joint-measurement uncertainty. Here, we implement the simplest possible technique for an optimal four-outcome joint measurement and demonstrate a type of optimal measurement that has not been realized before in a photonic setting. We experimentally investigate a joint-measurement uncertainty relation that is more fundamental in the sense that it refers only to probabilities and is independent of values assigned to measurement outcomes. Using a heralded single-photon source, we demonstrate quantum-limited performance of the scheme on single quanta. Since quantum measurements underpin many concepts in quantum information science, this study is both of fundamental interest and relevant for emerging photonic quantum technologies.

https://doi.org/10.1364/OPTICA.6.000257

1. INTRODUCTION

There are several types of uncertainty relations in quantum mechanics. To start with, if two noncommuting observables are each measured separately and sharply [1], then the product of their variances is bounded from below as specified by uncertainty relations [2–4]. In addition, measurements generally disturb a measured quantum state. This leads to further limitations on how well two observables can be measured *jointly* on the *same* quantum system. Different criteria for exactly what is to be optimized lead to different uncertainty or trade-off relations for joint measurements; see, e.g. [2,5–13].

Uncertainty relations apply to measurements of any noncommuting observables, such as position and momentum, and spin-1/2 (qubit) observables. Aside from their fundamental interest, uncertainty relations are relevant for quantum technology, including for quantum state estimation and quantum metrology. For example, they limit how much we can learn about different properties of quantum systems and are related to why one can bound the information held by an eavesdropper in quantum key distribution.

In this paper, we present the realization of a trade-off relation for joint measurements of a spin-1/2 system, given in Refs. [11,12]. Our realization uses the polarization of heralded single photons. Several experimental tests of different kinds of uncertainty relations for joint measurements have been reported; see, for example [14–20]. Some realizations have used weak measurements. Generally, however, any optimal quantum measurement will necessarily be described by a specific generalized quantum measurement [probability operator measure (POM) or positive-operator valued measure (POVM)], which in principle can always be realized in a single shot, with no need to resort to the framework of weak measurements or postselection. In fact, the joint measurement to saturate the uncertainty relations demonstrated in some of these previous works could also be realized as a single projective measurement [21]. Joint measurements can also be accomplished through quantum cloning [22,23]. This usually requires entangling operations, thereby imposing practical limitations, e.g., for photonic quantum technologies where deterministic entangling gates are lacking.

One might also expect that in order to realize a joint measurement of two noncommuting observables, it would be necessary to couple the quantum system to be measured to an ancillary system. For two qubit observables, however, it turns out that this is not necessary, and that an optimal measurement can be implemented by probabilistically selecting to perform one or the other of two projective measurements [24]. Such a setup was also suggested for measurement along two orthogonal spin directions in Refs. [25,26]. This leads to the simplest possible realization of an optimal joint measurement, requiring no entangling operations, and is therefore

the technique we employ here. In spite of its simplicity, this type of optimal joint measurement has not been realized before in a photonic setting.

An early example of a trade-off relation for joint measurements was given in Refs. [11,12]. This relation holds for measurements on spin-1/2 systems. A related relation [13] has been experimentally realized on a single trapped ion [20]. Here, we aim to test the original relation given in Refs. [11,12] using single photons.

2. THEORETICAL FRAMEWORK

We consider the joint measurement of a pair of noncommuting polarization components of a single photon. This is equivalent to measurements on a spin-1/2 quantum system along two nonorthogonal spin directions, say **a** and **b**, which are unit vectors on the Bloch sphere. In terms of photon polarization, this is equivalent to simultaneously measuring two polarization observables, where sharp measurements of these two observables correspond to projections in the orthonormal bases $\{|a\rangle, |a^{\perp}\rangle\}$ and $\{|b\rangle, |b^{\perp}\rangle\}$, respectively. In Fig. 1, we illustrate this on a Poincaré sphere which is the polarization equivalent of the Bloch sphere.

If spin-1/2 is sharply measured along the direction **a**, then the measurement operators are projectors and can be written as

$$P^{a}_{\pm} = \frac{1}{2}(\hat{\mathbf{1}} \pm \mathbf{a}\cdot\hat{\sigma}), \tag{1}$$

and similarly for **b**. In this case, the measurements are said to be *sharp*. In Refs. [11,12], the joint measurement is assumed to have marginal measurement operators of the form

$$\Pi^{a}_{\pm} = \frac{1}{2}(\hat{\mathbf{1}} \pm \alpha\mathbf{a}\cdot\hat{\sigma}), \quad \Pi^{b}_{\pm} = \frac{1}{2}(\hat{\mathbf{1}} \pm \beta\mathbf{b}\cdot\hat{\sigma}), \tag{2}$$

for the jointly measured spin-1/2 observables $\hat{A} = \mathbf{a}\cdot\hat{\sigma}$ and $\hat{B} = \mathbf{b}\cdot\hat{\sigma}$. It always holds that $0 \le \alpha, \beta \le 1$. If $\alpha = 1$, then $\Pi^{a}_{\pm}$ correspond to a projective measurement of $\mathbf{a}\cdot\hat{\sigma}$, while $\alpha = 0$ corresponds to a random guess, and similarly for $\Pi^{b}_{\pm}$. The coefficients α and β can be referred to as the *sharpnesses* of the measurements of $\mathbf{a}\cdot\hat{\sigma}$ and $\mathbf{b}\cdot\hat{\sigma}$, and the closer they are to 1, the sharper the measurements.

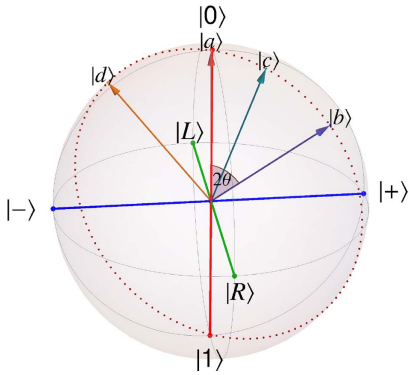

Fig. 1. Joint measurement of incompatible observables $\hat{A} = \mathbf{a}\cdot\hat{\sigma}$ and $\hat{B} = \mathbf{b}\cdot\hat{\sigma}$. The joint measurement is implemented by doing a projective measurement either of $\mathbf{c}\cdot\hat{\sigma}$ or of $\mathbf{d}\cdot\hat{\sigma}$, with probabilities p and $1-p$, respectively, where **c** and **d** will lie in the plane defined by **a** and **b**. The measurements correspond to projective measurements of photon polarization in appropriate bases. Here $\mathbf{a}, \mathbf{b}, \mathbf{c}, \mathbf{d}$ are Bloch vectors, denoted in the figure using ket representations of the corresponding polarization states $|a\rangle$, $|b\rangle$, $|c\rangle$, $|d\rangle$; each Bloch vector of unit length corresponds to a pure state.

A. Sharpness Trade-Off Relation

The trade-off relation for α and β given in Refs. [11,12] is

$$|\alpha\mathbf{a} + \beta\mathbf{b}| + |\alpha\mathbf{a} - \beta\mathbf{b}| \le 2, \tag{3}$$

which can be rewritten as [24]

$$\Delta^2_{\alpha}\Delta^2_{\beta} \equiv \frac{(1-\alpha^2)(1-\beta^2)}{\alpha^2\beta^2} \ge \sin^2(2\theta), \tag{4}$$

where 2θ is the angle between **a** and **b**, and θ would be the angle between the equivalent polarization- or qubit-state vectors. The bound in Eqs. (3) and (4) is tight, in the sense that a joint quantum measurement with marginal measurement operators given by Eq. (2), for any α and β saturating the bound, can always be realized.

Note that the bound does not depend on the measured state, nor on what values we assign to the measurement outcomes. In this sense, the bound in Eqs. (3) and (4) can be said to be more "fundamental" than relations that depend on what values are assigned for measurement outcomes, which is the case for typical error-disturbance relations. In return, we assume that $\mathbf{a}\cdot\hat{\sigma}$ and $\mathbf{b}\cdot\hat{\sigma}$ are jointly measured using measurement operators of the form in Eq. (2). More generally, however, measurement operators for a joint measurement of $\mathbf{a}\cdot\sigma$ and $\mathbf{b}\cdot\sigma$ do not have to be of the form in Eq. (2) [8,13], in which case the bound in Eqs. (3) and (4) also retains its relevance.

In fact, any dichotomic spin-1/2 observable will have measurement operators of the form

$$\Pi_{\pm} = \frac{\gamma_{\pm}}{2}\hat{\mathbf{1}} \pm \frac{\gamma_k}{2}\mathbf{k}\cdot\hat{\sigma}, \tag{5}$$

where $\gamma_+, \gamma_- \ge \gamma_k$ (since measurement operators must be positive) and $\gamma_+ + \gamma_- = 1$ (since $\Pi_+ + \Pi_- = \hat{\mathbf{1}}$ must hold). Thus, the marginal measurement operators of a joint measurement must more generally be of this form. It turns out that if we choose $\gamma_+ = \gamma_- = 1/2$, then the measurement can be made sharper, in the sense that γ_k in the joint measurement is as large as possible, while keeping the direction **k** the same. Therefore, no matter what the measurement results are used to estimate, measurement operators of the form in Eq. (2) can be said to be optimal. In this sense, Eqs. (3) and (4) retain their relevance even more generally. Thus, they can be understood as underlying any other type of joint measurement, which, to our knowledge, is an interesting new insight. For example, in Ref. [13], one essentially ends up with measurement operators of the form Eq. (2), but for two "new" spin directions other than **a** and **b**, and hence one obtains a relation of the form in Eqs. (3) and (4), just for these two "new" spin directions.

We can also connect Eq. (4) with uncertainty relations. The total uncertainties in the joint measurement, denoted ΔA_j and ΔB_j, arise from two sources: the "intrinsic uncertainties" ΔA and ΔB in the quantum observables when they are measured sharply (measured separately, not jointly) on some quantum state, and "extra" uncertainty coming the fact that they are measured jointly. If we assume that the measurement results both for the sharp and the joint measurements are said to be ± 1, then the variance in the joint measurement of $\mathbf{a}\cdot\hat{\sigma}$, scaled with α^{-2}, can be written

$$\Delta^2 A_j/\alpha^2 = (1-\alpha^2\langle\hat{A}\rangle^2)/\alpha^2 = (1-\alpha^2)/\alpha^2 + 1 - \langle\hat{A}\rangle^2, \tag{6}$$

and similarly for $\Delta^2 B_j$ [27]. Here $1 - \langle\hat{A}\rangle^2 = \Delta^2 A$ is the variance of $\hat{A}$, when measured separately and sharply, and similarly for $\hat{B}$. The quantities $(1-\alpha^2)/\alpha^2 \equiv \Delta^2_{\alpha}$ and $(1-\beta^2)/\beta^2 \equiv \Delta^2_{\beta}$ are seen

to be contributions coming from the fact that the measurement is a joint measurement. A lower bound on their product is given by Eq. (4), which can now be interpreted as an uncertainty relation giving a lower bound on the uncertainty associated purely with the fact that quantum observables $\hat{A}$ and $\hat{B}$ are measured *jointly*.

B. Optimal Joint-Measurement Scheme

As shown in Ref. [24], it turns out that any optimal joint measurement along spin directions **a** and **b** can be realized by doing a projective measurement *either* along **c** or along **d** with probability p or $1-p$, respectively, as illustrated in Fig. 1. The results of the joint measurement are assigned as follows. If measurement along **c** is chosen, and the outcome is $C=+1$, then the result of the joint measurement is $A_j=+1$ and $B_j=+1$. If the outcome is $C=-1$, the result of the joint measurement is $A_j=-1$ and $B_j=-1$. However, if the selected measurement is along **d**, and the outcome is $D=+1$, then the result of the joint measurement is $A_j=+1$ and $B_j=-1$, while $D=-1$ corresponds to $A_j=-1$ and $B_j=+1$. Note that although the scheme involves a probabilistic selection between projective measurements, a measurement outcome would always be obtained for both of the jointly measured observables for every particle being measured. In this sense, this scheme is deterministic.

The expectation values for this joint measurement are then

$$\bar{A}_j = p\langle \mathbf{c}\cdot\hat{\sigma}\rangle + (1-p)\langle \mathbf{d}\cdot\hat{\sigma}\rangle,$$
$$\bar{B}_j = p\langle \mathbf{c}\cdot\hat{\sigma}\rangle - (1-p)\langle \mathbf{d}\cdot\hat{\sigma}\rangle. \tag{7}$$

On the other hand, the expectation values for a joint measurement with marginal measurement operators given by Eq. (2) are $\bar{A}_j=\alpha\langle \mathbf{a}\cdot\hat{\sigma}\rangle$ and $\bar{B}_j=\beta\langle \mathbf{b}\cdot\hat{\sigma}\rangle$. We therefore obtain

$$\mathbf{c}=\frac{(\alpha\mathbf{a}+\beta\mathbf{b})}{2p} \quad \text{and} \quad \mathbf{d}=\frac{(\alpha\mathbf{a}-\beta\mathbf{b})}{2(1-p)}. \tag{8}$$

Since $\mathbf{c},\mathbf{d}$ are unit vectors, it holds that

$$p=|(\alpha\mathbf{a}+\beta\mathbf{b})|/2$$
$$1-p=|(\alpha\mathbf{a}-\beta\mathbf{b})|/2. \tag{9}$$

Adding these two equations, we see that this measurement satisfies equality in Eq. (3), meaning that the joint measurement realized through measuring either $\hat{C}=\mathbf{c}\cdot\hat{\sigma}$ or $\hat{D}=\mathbf{d}\cdot\hat{\sigma}$ with probabilities p and $1-p$ is indeed optimal.

Solving Eq. (9) and using equality in Eq. (4), we can express the corresponding optimal α and β in terms of θ and p as

$$\alpha_{\text{opt}}=\frac{(2p-1)}{\beta_{\text{opt}}\cos(2\theta)}, \quad \text{where}$$
$$\beta_{\text{opt}}=\pm\Bigg\{\sqrt{\pm[2(p-1)p+1]^2-(1-2p)^2\sec^2(2\theta)} + 2(p-1)p+1\Bigg\}^{\frac{1}{2}}. \tag{10}$$

An intuitive understanding of the sharpness relation and the optimal choices of **c** and **d** for realizing the joint measurement can be gained by considering a parallelogram whose sides are the noncollinear vectors $\alpha\mathbf{a}$ and $\beta\mathbf{b}$. For a joint measurement of spin along both **a** and **b** to be possible, then according to Eq. (3), the sum of the diagonals of this parallelogram must be less than 2, forcing $|\alpha|,|\beta|<1$, since **a** and **b** are unit vectors. This is the essence and simple geometrical meaning of the bound in relations (3, 4). This bound is saturated when **c** and **d** are chosen such that the diagonals of this parallelogram are $2p\mathbf{c}$ and $2(1-p)\mathbf{d}$, since this maximizes α, β. Also, for measurement along both **a** and **b**, it makes intuitive sense that it would be useful to measure along a direction that lies somewhere between, as a "compromise" between **a** and **b**. Measuring each quantum system along either **c** or **d** is better than measuring either along **a** or along **b** in the sense that the latter cannot saturate relations (3, 4) as proven in Refs. [11,12].

3. EXPERIMENT

The schematic of the experimental measurement setup realizing the strategy is shown in Fig. 2. We prepare the input state using a combination of wave plates (not shown) on the input arm before the beam splitter, and implement the random selection between measurement directions **c**, **d** using a fixed, nonpolarizing beam splitter with a splitting ratio corresponding to $p\sim 0.7$. The reason for choosing $p\sim 0.7$ is that this choice allows us to investigate a range of angles between the directions **a** and **b** by varying the directions **c** and **d**. In return, the maximum possible angle between **a** and **b** we can achieve is about $2\theta=50°$. If one would want to perform a joint measurement of maximally complementary observables, this can only be achieved with $p=1/2$. Conversely, $p=1/2$ would always result in a measurement of two maximally complementary spin-1/2 observables; by varying

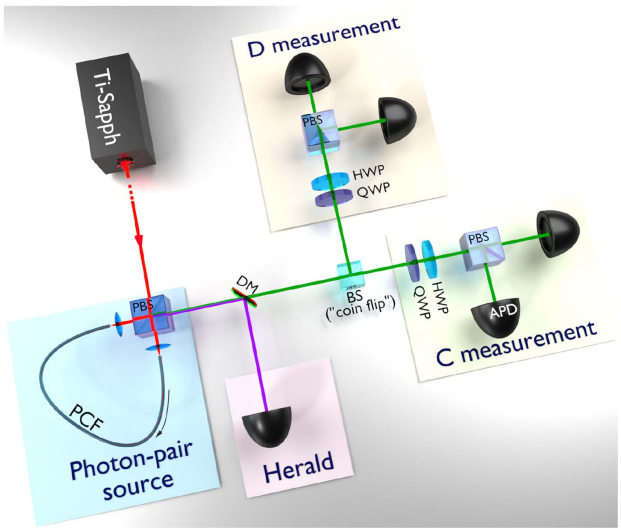

Fig. 2. Schematic of experimental realization of a deterministic scheme for joint quantum measurements: Single signal photons (623 nm) heralded by idler photons (871 nm) were generated from a four-wave mixing source in a PCF pumped at 726 nm. To realize the joint measurement of observables $\mathbf{a}\cdot\hat{\sigma}$ and $\mathbf{b}\cdot\hat{\sigma}$, the signal photons, prepared in a well-defined polarization state, are measured in either a polarization basis corresponding to a measurement of $\mathbf{c}\cdot\hat{\sigma}$ or to that of $\mathbf{d}\cdot\hat{\sigma}$, with probabilities $p, 1-p$, respectively. The random selection probability corresponding to the splitting ratio of the beam splitter is $p\sim 0.7$, but could also be implemented with a flip of an unbalanced classical coin. The source generates photon pairs cross-polarized to the pump, which are filtered by both the PBS and additional wideband filters (not shown), resulting in pure horizontally polarized heralded photons entering the measurement stage. Components: pulsed laser (Ti:Sapph), half-wave plate (HWP), quarter-wave plate (QWP), polarizing beam splitter (PBS), non-polarizing beam splitter (BS), dichroic mirror (DM), multimode-fiber-coupled single-photon avalanche diode (APD).

the directions **c** and **d**, one can in that case vary the relative sharpnesses of the measurements of $\mathbf{a}\cdot\hat{\sigma}$ and $\mathbf{b}\cdot\hat{\sigma}$ in the joint measurement.

To determine the optimal measurement directions **c** and **d**, we solve Eq. (9) for α, β satisfying equality in Eq. (4) for each combination of **a**, **b**. For each **a**, **b**, we then use these solutions α_{opt}, β_{opt}, i.e., Eq. (10), in Eq. (8) to get the **c**, **d** that are subsequently used as the measurement settings. Of course, due to experimental imperfections, the actual experimental values $\alpha_{\text{exp}}, \beta_{\text{exp}}$ determined from the measurements of **c**, **d** chosen in this way may not necessarily saturate the bound in Eq. (4). However, we are able to saturate this bound within experimental error bars from Poissonian photon counting statistics. Note that for this scheme it would suffice to use a classical random selection of the measurement, and this is equivalent to the flip of an unbalanced classical coin.

We perform three sets of experiments using pairs **a**, **b**, with **a** kept constant as the **z** direction, and varying **b** to traverse $\theta = 1, \ldots, 25°$, along a different plane on the Bloch sphere for each experiment corresponding to azimuthal angles $\phi_1 = -160.7°$, $\phi_2 = -51.6°$, $\phi_3 = 83.7°$, for experiments 1, 2, and 3, respectively. For our experiments, we chose as input state the eigenstate of $\mathbf{a}\cdot\hat{\sigma}$, denoted $|a\rangle$, which coincides with the "$|0\rangle$" state. To experimentally estimate how sharp a measurement of a single observable is, then intuitively, it would be best to measure eigenstates of that observable. Conversely, if the measured state is an eigenstate of a complementary observable, or is a maximally mixed state, then no matter how sharp the measurement is, the measurement result is random, and we can make no good estimate of the measurement's sharpness. When estimating how sharp a joint measurement of two incompatible observables is, however, it is not intuitively clear what the best (single) state to measure is, in order to minimize the error in the experimental estimate of both sharpnesses, defined in some reasonable way. Which probe state gives an optimal estimate is in fact an interesting question, which we plan to address in future work. Here, an eigenstate of one of the observables is simply one possible choice. It is a natural choice since this would at least be optimal for estimating the sharpness of that observable, even if it is not optimal for the other. [see Fig. 3(a)]. We carry out the measurements of $\mathbf{c}\cdot\hat{\sigma}$ and $\mathbf{d}\cdot\hat{\sigma}$, by measuring in the corresponding polarization bases using appropriate settings of the half-wave plates and quarter-wave plates and subsequent measurement in the $\{|H\rangle, |V\rangle\}$ polarization basis using a polarizing beam splitter and fiber-coupled single-photon detectors. Using coincidence detection with idler photons as heralds, we are able to register any of the four possible outcomes for each heralded photon going through the measurement circuit (see Fig. 2).

4. METHODS

We ensure a true single-photon implementation by exploiting a heralded source of single photons consisting of a microstructured photonic crystal fiber (PCF) exploiting birefringent phase-matching [28,29] to produce photon pairs via spontaneous four-wave mixing (SFWM). This source is pumped by a pulsed Ti:Sapphire laser with a repetition rate of 80 MHz. The fiber is highly birefringent ($\Delta n = 4 \times 10^{-4}$) with phase-matching conditions leading to generation of signal-idler pairs with polarization orthogonal to that of the pump. In addition to this birefringence, the waveguide contributions to the dispersion can be used to tailor

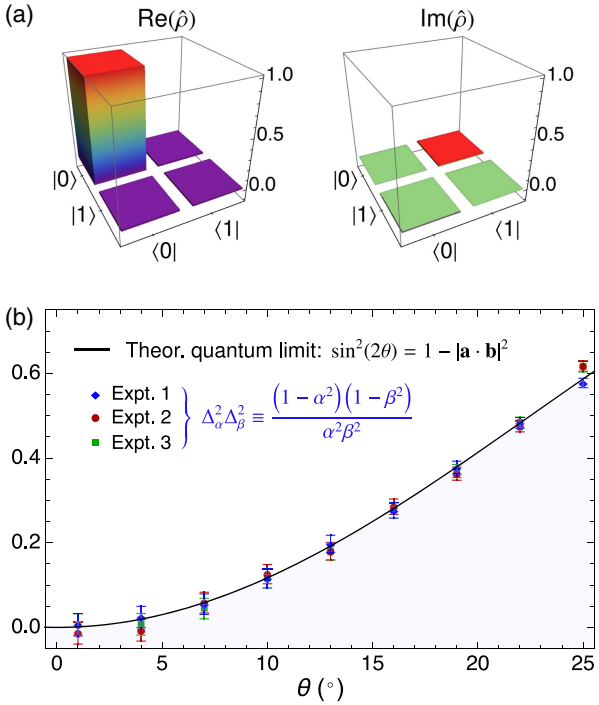

Fig. 3. Experimental results. (a) Input state tomography. Tomography has been performed in the "C measurement" arm of the apparatus as well as the "D measurement" arm on the same input state $|0\rangle$, each resulting in a state preparation fidelity of $\mathcal{F}_p = 99.5\%$. The fidelity between the two resulting state reconstructions is $\mathcal{F}_c = 99.9993(2)\%$, indicating that the measurement setups are well calibrated to each other. (b) Sharpness of the joint measurement. The quantity on the left-hand side of Eq. (4) as a function of $\theta = \arccos(|\mathbf{a}\cdot\mathbf{b}|)/2$, i.e., $\Delta_\alpha^2\Delta_\beta^2$, which represents the contribution to measurement uncertainty *purely due to performing the measurements jointly*. The error bars are determined only by Poisson statistics of raw count rates. The plot shows three sets of experiments, each corresponding to **a**, **b** defining a distinct plane on the Bloch sphere (see Fig. 5). Each data point is an average of 100 runs, each of which involved the detection of $\sim 1.5 \times 10^4$ heralded single photons. The solid black line represents the quantum limit.

the SFWM for generation of naturally narrowband, spectrally uncorrelated photons when pumped with Ti:Sapphire laser pulses at the flat region of the phase-matching curves ($\lambda_{\text{pump}} \simeq 726$ nm) where the idler photons ($\lambda_i = 871$ nm) are group-velocity-matched to the pump pulse so that they become spectrally broad ($\Delta\lambda_i = 2.2$ nm), while the signal photons ($\lambda_s = 623$ nm) are intrinsically narrowband ($\Delta\lambda_s = 0.3$ nm). This narrowband phase-matching results in a highly separable joint-spectral amplitude for a wide range of pump bandwidths, thereby enabling the generation of single photons of high state purity. Although the fiber source is in a Sagnac-loop configuration, allowing for generation of entangled states when the pump pulse is set to diagonal polarization and split at the polarizing beam splitter (Fig. 2), we use horizontally polarized pump pulses so that the PCF is pumped in only one direction for use as a heralded single-photon source.

5. RESULTS

Let the heralded detector count rates corresponding to $\mathbf{c}\cdot\hat{\sigma} \equiv C = \pm 1$ and $\mathbf{d}\cdot\hat{\sigma} \equiv D = \pm 1$ be $\mathcal{C}_\pm$ and $\mathcal{D}_\pm$, respectively. From these, we determine the experimental expectation values as

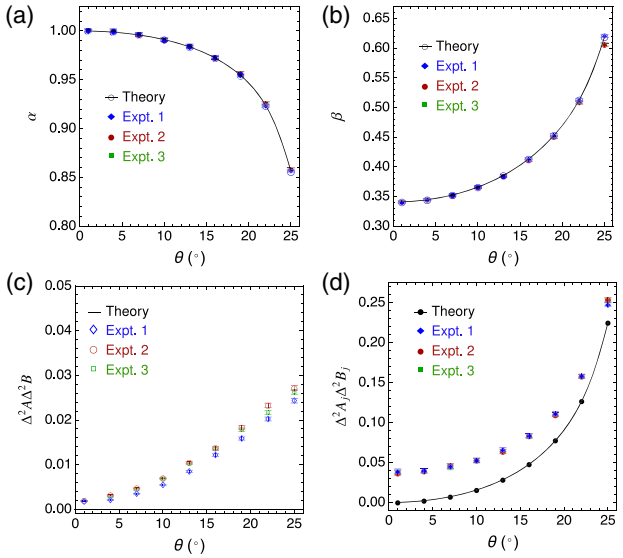

Fig. 4. Experimental values of (a) α and (b) β as functions of θ, plotted with the corresponding theoretical values; (c) product of experimental variances for the sharp measurements; (d) product of experimental variances for the joint measurements and their comparison with theory for the ideal case and infinite number of runs of the experiment.

$$\langle \hat{C} \rangle = \frac{\mathcal{C}_+ - \mathcal{C}_-}{\mathcal{C}_+ + \mathcal{C}_-}, \qquad \langle \hat{D} \rangle = \frac{\mathcal{D}_+ - \mathcal{D}_-}{\mathcal{D}_+ + \mathcal{D}_-}. \tag{11}$$

Using this in Eq. (7), and using the value of $p = 0.670(1)$ obtained from total count rates in the C and D channels, the experimental joint-measurement expectations values $\bar{A}_j, \bar{B}_j$ are then obtained directly according to Eq. (7).

To benchmark the performance of the implemented joint measurements, we also perform separate sharp measurements of the incompatible observables $\mathbf{a} \cdot \hat{\sigma}$, $\mathbf{b} \cdot \hat{\sigma}$. Again, if we denote the detector count rates corresponding to $A = \pm 1$ and $B = \pm 1$ as $\mathcal{A}_\pm$ and $\mathcal{B}_\pm$, respectively, the expectations values for the sharp measurements are

$$\langle \mathbf{a} \cdot \hat{\sigma} \rangle = \frac{\mathcal{A}_+ - \mathcal{A}_-}{\mathcal{A}_+ + \mathcal{A}_-}, \qquad \langle \mathbf{b} \cdot \hat{\sigma} \rangle = \frac{\mathcal{B}_+ - \mathcal{B}_-}{\mathcal{B}_+ + \mathcal{B}_-}. \tag{12}$$

This allows us to obtain experimental values of α, β as

$$\alpha = \overline{A_j} / \langle \mathbf{a} \cdot \hat{\sigma} \rangle, \qquad \beta = \overline{B_j} / \langle \mathbf{b} \cdot \hat{\sigma} \rangle, \tag{13}$$

which directly indicates by how much the sharpnesses are worsened *solely by the fact that the measurement is joint*. From α, β we evaluate the left-hand side of relation Eq. (4), which we plot as a function of θ in Fig. 3(b) as our main result.

Figures 4(a), 4(b) and 4(c), 4(d) show α, β and the product of total variances for separate (sharp) and joint measurements, respectively. The ideal theoretical product of total "intrinsic" variances for sharp measurements is zero, as indicated by the solid black line in Fig. 4(c), since the measured state is an eigenstate of $\mathbf{a} \cdot \hat{\sigma}$, while that for the joint measurements (determined by the incompatibility of the jointly measured observables, and parameterized by θ) is plotted with the black filled circles in Fig. 4(d). Figure 5 shows examples of pairs of spin directions $\mathbf{a}, \mathbf{b}, \mathbf{c}, \mathbf{d}$ used in the sets of experiments. Also, shown in Fig. 6 are the expectation values for the individual "sharp" measurements of $\mathbf{a} \cdot \hat{\sigma}$,

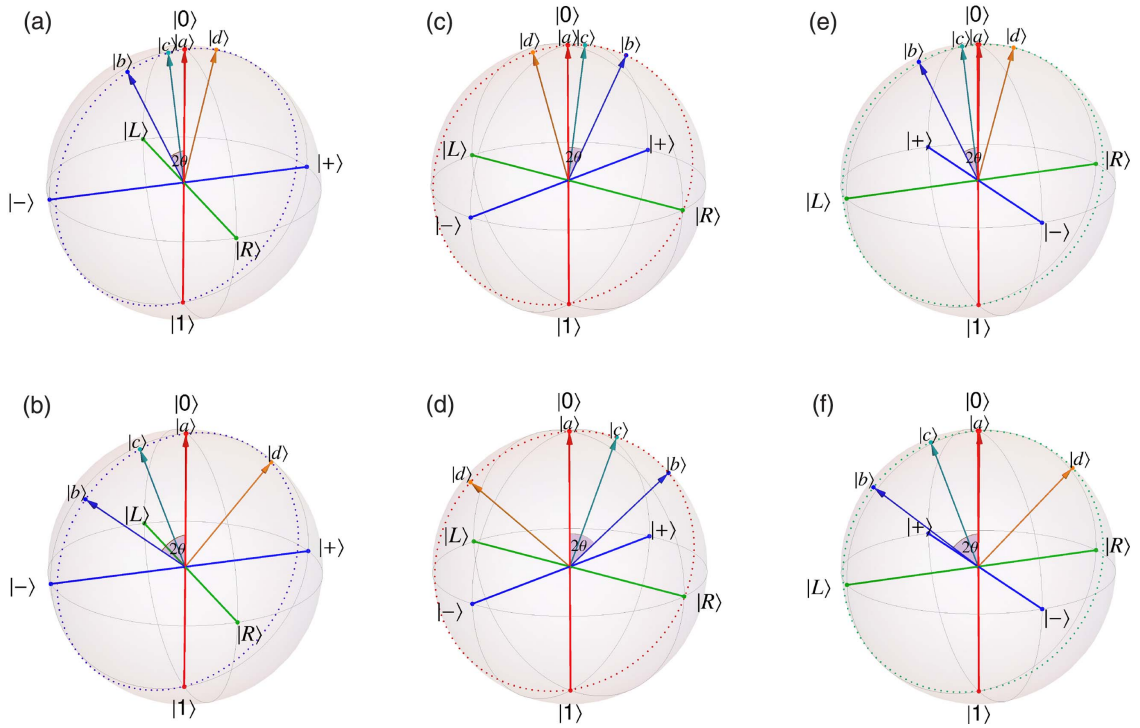

Fig. 5. Examples of pairs of incompatible observables used in the experiments. Spin directions $\mathbf{a}$, $\mathbf{b}$ (states $|a\rangle$, $|b\rangle$) defining the incompatible observables, along with $\mathbf{c}$, $\mathbf{d}$ (states $|c\rangle$, $|d\rangle$) for implementing their joint measurements with (a) $\theta = 13°$ in experiment 1, (b) $\theta = 25°$ in experiment 1, (c) $\theta = 13°$ in experiment 2, (d) $\theta = 25°$ in experiment 2, (e) $\theta = 13°$ in experiment 3, (f) $\theta = 25°$ in experiment 3. For the experiments, $\mathbf{a}$ is kept constant, and $\mathbf{b}$ is varied such that $\theta \equiv \arccos(|\mathbf{a} \cdot \mathbf{b}|)/2 = 1, 4, 7, \ldots, 25°$, for each of the three sets of experiments, corresponding to azimuthal angles $\phi_1 = -160.7°$, $\phi_2 = -51.6°$, $\phi_3 = 83.7°$, for experiments 1, 2, and 3, respectively.

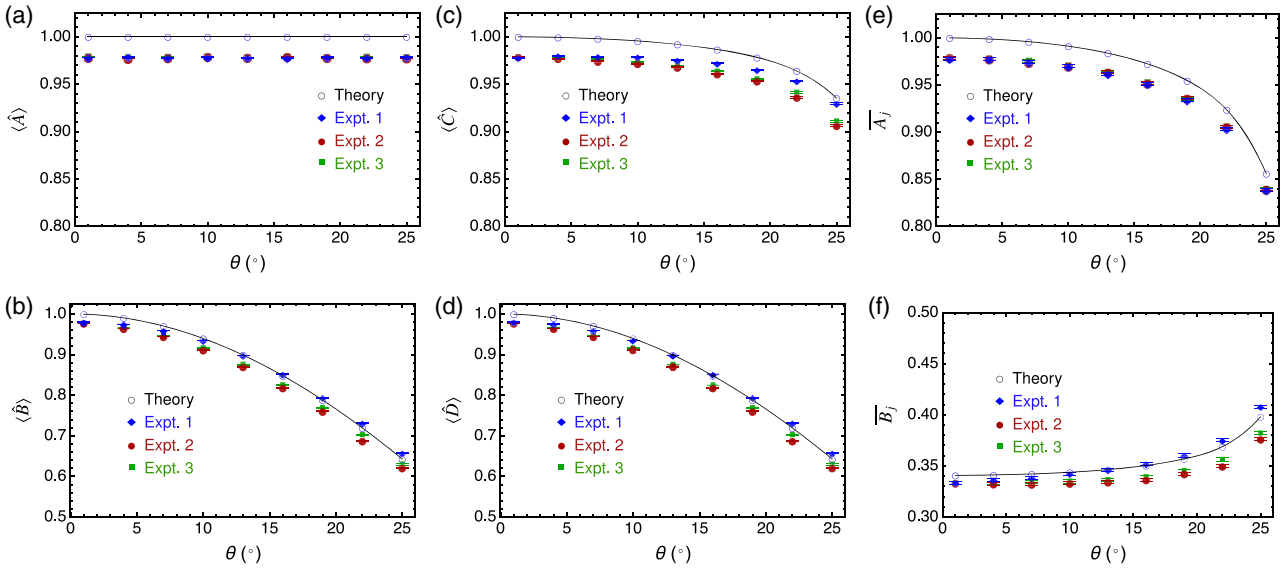

Fig. 6. Expectation values for the individual "sharp" and joint measurements. For the three experiments, the plots show expectation values for sharp measurements of (a) $\mathbf{a}\cdot\hat{\sigma}$ and (b) $\mathbf{b}\cdot\hat{\sigma}$, (c) $\mathbf{c}\cdot\hat{\sigma}$ and (d) $\mathbf{d}\cdot\hat{\sigma}$, and expectation values for the joint measurements (e) $\overline{A_j}$ and (f) $\overline{B_j}$. Also plotted for comparison are the ideal theoretical predictions, which do not include the effects of experimental imperfections.

$\mathbf{b}\cdot\hat{\sigma}$, and expectation values resulting from the implemented joint-measurement strategy.

6. DISCUSSION

The nonideal experimental values of the sharp measurement variances $\Delta^2A\Delta^2B$, rather than the implementation of the joint measurement strategy, is accountable for the deviation of the $\Delta^2A_j\Delta^2B_j$ from the ideal value because, as seen in Fig. 3, the contribution purely due to the jointedness of the measurement is at the quantum limit. Although achieving ideal values of sharp measurement variances would be a much more daunting task and is not the goal of this work, we see that, even without making any other corrections for experimental imperfections, our results verge on the quantum mechanical limit of how much variances must increase *due to performing the quantum measurements jointly*. Indeed, our main result can be rephrased as saying that while there is additional variance in the measured results, over and above what is strictly possible, none of the additional variance comes from the fact that the measurement is joint. This is thanks to the simplicity of the scheme, the brightness of the heralded single-photon source that reduced the effect of Poissonian noise, and the precise calibration of the two measurement setups with each other with a fidelity of $\mathcal{F}_c = 99.9993(2)\%$. Note that this does not refer to the state preparation fidelity ($\mathcal{F}_p = 99.5\%$), nor the fidelity of an individual measurement device. Rather, it refers to how identical the results of their individual tomographic measurements of the same input state are. We emphasize that the quantity $\Delta_\alpha^2\Delta_\beta^2$ is extremely sensitive to experimental error, e.g., as quantified by F_c, and has no upper bound.

A true joint measurement of two observables performed on a single qubit or spin-1/2 system should have four possible outcomes for each qubit measured, as is now demonstrated here. Although we test the optimality of our measurements in terms of the sharpness uncertainty relation, the kind of technique we implement can be used to saturate any other types of trade-off relations (such as entropic uncertainty relations [30]) with appropriate choices of coin flip probabilities and measurement settings. In particular, the simple experimental setup used in our work is more generally applicable, as it can be used to saturate both the Branciard relations [21] (with a single projective measurement by setting $p = 1$) and the Busch–Lahti relation [11,12], which is the one we test here. In contrast to the Branciard relation, a single projective measurement is not enough to saturate the Busch–Lahti relation. Furthermore, it is not well known that the Busch–Lahti sharpness relation in Eqs. (3), (4) is also a valid way of defining what a joint measurement is, nor that it can be realized in such a simple way.

In conclusion, we have demonstrated an optimal joint measurement scheme that does not use filtering or postselection, nor does it need entangling interactions with an ancilla. In addition, it is elegantly simple and robust to realize experimentally. As discussed in connection with Eq. (5), the joint measurement relation we test can also be said to be relevant to other types of optimal joint measurements, but for some other suitably chosen directions **a**, **b**, and suitable α, β. The implemented scheme can easily be applied to other qubit degrees of freedom and other two-level quantum systems, since standard projective measurements and flips of unbalanced classical "coins" are generally easy to implement. It would be of interest to extend this scheme to joint measurement of incompatible observables of higher-dimensional systems (qudits), or of multiple incompatible observables. This work demonstrates how to fully implement joint measurements of noncommuting spin-1/2 (or qubit) observables in an optimal way, and with fewer quantum resources than often employed in previous implementations.

Funding. Engineering and Physical Sciences Research Council (EPSRC) (EP/L024020/1, EP/M024156/1, EP/M024458/1, EP/N003381/1); European Commission (EC) (FP7-284743).

REFERENCES AND NOTES

1. What is meant by a "sharp" measurement is when an observable is measured by making a projective measurement in its eigenbasis.
2. W. Heisenberg, "Über den anschaulichen inhalt der quantentheoretischen kinematik und mechanik," Zeitschrift für Physik A Hadrons and Nuclei **43**, 172–198 (1927).
3. H. P. Robertson, "The uncertainty principle," Phys. Rev. **34**, 163–164 (1929).
4. E. Schrödinger, "About Heisenberg uncertainty relation," Sitzungsber. Preuss. Akad. Wiss. Berlin (Math. Phys.) **19**, 296–303 (1930).
5. E. Arthurs and J. Kelly, Jr., "On the simultaneous measurement of a pair of conjugate observables," Bell Syst. Tech. J. **44**, 725–729 (1965).
6. E. Arthurs and M. Goodman, "Quantum correlations: a generalized Heisenberg uncertainty relation," Phys. Rev. Lett. **60**, 2447–2449 (1988).
7. S. Stenholm, "Simultaneous measurement of conjugate variables," Ann. Phys. **218**, 233–254 (1992).
8. M. J. Hall, "Prior information: how to circumvent the standard joint-measurement uncertainty relation," Phys. Rev. A **69**, 052113 (2004).
9. M. Ozawa, "Universally valid reformulation of the Heisenberg uncertainty principle on noise and disturbance in measurement," Phys. Rev. A **67**, 042105 (2003).
10. P. Busch, P. Lahti, and R. F. Werner, "Proof of Heisenberg's error-disturbance relation," Phys. Rev. Lett. **111**, 160405 (2013).
11. P. Busch, "Unsharp reality and joint measurements for spin observables," Phys. Rev. D **33**, 2253–2261 (1986).
12. P. Busch, M. Grabowski, and P. J. Lahti, *Operational Quantum Physics* (Springer, 2001).
13. P. Busch, P. Lahti, and R. F. Werner, "Heisenberg uncertainty for qubit measurements," Phys. Rev. A **89**, 012129 (2014).
14. J. Erhart, S. Sponar, G. Sulyok, G. Badurek, M. Ozawa, and Y. Hasegawa, "Experimental demonstration of a universally valid error-disturbance uncertainty relation in spin measurements," Nat. Phys. **8**, 185–189 (2012).
15. M. M. Weston, M. J. Hall, M. S. Palsson, H. M. Wiseman, and G. J. Pryde, "Experimental test of universal complementarity relations," Phys. Rev. Lett. **110**, 220402 (2013).
16. G. Sulyok, S. Sponar, J. Erhart, G. Badurek, M. Ozawa, and Y. Hasegawa, "Violation of Heisenberg's error-disturbance uncertainty relation in neutron-spin measurements," Phys. Rev. A **88**, 022110 (2013).
17. L. A. Rozema, A. Darabi, D. H. Mahler, A. Hayat, Y. Soudagar, and A. M. Steinberg, "Violation of Heisenberg's measurement-disturbance relationship by weak measurements," Phys. Rev. Lett. **109**, 100404 (2012).
18. M. Ringbauer, D. N. Biggerstaff, M. A. Broome, A. Fedrizzi, C. Branciard, and A. G. White, "Experimental joint quantum measurements with minimum uncertainty," Phys. Rev. Lett. **112**, 020401 (2014).
19. F. Kaneda, S.-Y. Baek, M. Ozawa, and K. Edamatsu, "Experimental test of error-disturbance uncertainty relations by weak measurement," Phys. Rev. Lett. **112**, 020402 (2014).
20. T. Xiong, L. Yan, Z. Ma, F. Zhou, L. Chen, W. Yang, M. Feng, and P. Busch, "Optimal joint measurements of complementary observables by a single trapped ion," New J. Phys. **19**, 063032 (2017).
21. C. Branciard, "Error-tradeoff and error-disturbance relations for incompatible quantum measurements," Proc. Natl. Acad. Sci. USA **110**, 6742–6747 (2013).
22. T. Brougham, E. Andersson, and S. M. Barnett, "Cloning and joint measurements of incompatible components of spin," Phys. Rev. A **73**, 062319 (2006).
23. G. Thekkadath, R. Saaltink, L. Giner, and J. Lundeen, "Determining complementary properties with quantum clones," Phys. Rev. Lett. **119**, 050405 (2017).
24. E. Andersson, S. M. Barnett, and A. Aspect, "Joint measurements of spin, operational locality, and uncertainty," Phys. Rev. A **72**, 042104 (2005).
25. P. Busch, "Some realizable joint measurements of complementary observables," Found. Phys. **17**, 905–937 (1987).
26. S. M. Barnett, "Quantum information via novel measurements," Philos. Trans. R. Soc. London, Ser. A **355**, 2279–2290 (1997).
27. Equivalently, we can assume that the measurement results are $\pm 1/\alpha$.
28. M. Halder, J. Fulconis, B. Cemlyn, A. Clark, C. Xiong, W. J. Wadsworth, and J. G. Rarity, "Nonclassical 2-photon interference with separate intrinsically narrowband fibre sources," Opt. Express **17**, 4670–4676 (2009).
29. A. Clark, B. Bell, J. Fulconis, M. M. Halder, B. Cemlyn, O. Alibart, C. Xiong, W. J. Wadsworth, and J. G. Rarity, "Intrinsically narrowband pair photon generation in microstructured fibres," New J. Phys. **13**, 065009 (2011).
30. A. A. Abbott and C. Branciard, "Noise and disturbance of qubit measurements: an information-theoretic characterization," Phys. Rev. A **94**, 062110 (2016).